ISBN: 978-3-95450-191-5 doi:10.18429/JACoW-SRF2017-THPB053

SURFACE RESISTANCE CHARACTERIZATION OF Nb_3Sn USING THE HZB QUADRUPOLE RESONATOR

S. Keckert*, O. Kugeler, J. Knobloch, Helmholtz-Zentrum Berlin, Berlin, Germany
D. L. Hall, M. Liepe, Cornell University, Ithaca, USA

Abstract

Nb_3Sn is a very promising candidate material for future SRF cavities. With a critical temperature more than twice as the one of bulk niobium, higher operational temperatures with still lower surface resistance are theoretically possible. The RF properties of a sample prepared by Cornell University were characterized using the HZB Quadrupole Resonator. In comparison to a coated cavity this device enables SRF measurements over an extended parameter space (frequency, temperature and RF field) and easy access to physical quantities such as critical field and penetration depth. In this contribution we present surface resistance and RF critical field measurements.

INTRODUCTION

Nb_3Sn is one of the most promising alternative materials to niobium for applications in SRF cavities. With its high critical temperature of about 18.5 K and superheating critical field $B_{sh} \approx 400\,\mathrm{mT}$ [1], Nb_3Sn provides potential major improvements for both applications currently being investigated in the SRF community, high gradient accelerators as well as high-Q cavities with significantly reduced operating costs. Recent results with cavities have demonstrated R_s values of about 27 nΩ at 4.2 K far beyond the fundamental limit of niobium [2].

Sample Preparation

The sample characterized in this work was prepared at Cornell University using the coating procedure commonly applied to single cell cavities [2, 3]. As substrate a RRR 300 fine grain bulk niobium QPR sample was used. Prior to coating the substrate was characterized at HZB showing very good residual resistance of about 4 nΩ and high RF critical field $B_{c,RF} = 220\,\mathrm{mT}$ [4].

For coating the substrate is placed into a UHV furnace with a $SnCl_2$ tin source inside. The process starts with heating up to 500 °C where tin evaporates from the source and forms nucleation sites on the niobium substrate. The actual coating consisting of diffusion of tin into niobium along with alloying to Nb_3Sn happens at a substrate temperature of 1100 °C with the source heated even further to 1200 °C. After 3 hours of coating the source heater is switched off while the sample is kept at high temperature for approximately 6.5 hours in order to allow for further annealing and grain growth.

* sebastian.keckert@helmholtz-berlin.de

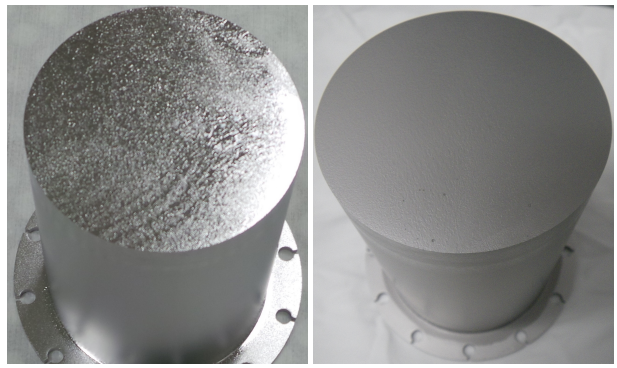

Figure 1: QPR sample before (left) and after (right) coating with Nb_3Sn.

EXPERIMENTAL SETUP: THE QUADRUPOLE RESONATOR

At HZB a Quadrupole Resonator (QPR) is available which enables SRF characterization of planar samples in a wide parameter space of temperature, RF field strength and frequency [5–7]. Up to now the sample had to be brazed into a stainless steel flange prior to mounting into the resonator. This joint limited the maximum temperature available for sample treatments to few hundred °C. Alternatively, brazing or an electron-beam weld had to be made after sample treatment which itself could affect relevant material properties. In order to allow for high temperature treatments of the sample – such as coating with Nb_3Sn – a modified sample chamber was developed [4]. In addition to available treatments this design makes samples exchangeable between the two existing QPRs at CERN and HZB. The main part as depicted in Fig. 1 is mounted into a double-sided CF100 flange using an indium wire gasket. This assembly is then inserted into the resonator (Fig. 2). As before, the planar surface on

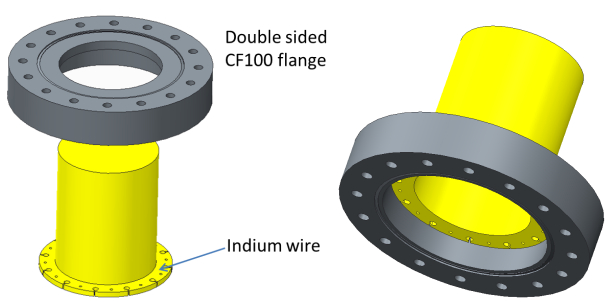

Figure 2: CAD sketch of the newly developed QPR sample chamber. Exploded view (left) and assembly ready for mounting into the QPR (right).

ISBN: 978-3-95450-191-5 doi:10.18429/JACoW-SRF2017-THPB053

top of the assembly (∅ 75 mm) constitutes the actual sample surface which is exposed to the RF field. Inside the QPR the sample chamber acts as the inner conductor of a coaxial structure operated below cutoff for the quadrupole mode. The outer surface of the cylindrical part has to be coated as well, since only then the contribution of that surface to the RF losses is negligible.

Right below the RF surface the sample is equipped with a DC heater and calibrated Cernox temperature sensors. Using a PID control loop with one Cernox sensor as feedback, the sample temperature can be varied and stabilized. At all times during measurements the temperature of the helium bath surrounding the QPR is kept constant at 1.8 K. Due to the long thermal path the sample is decoupled from the resonator so that a calorimetric measurement of the RF surface resistance is possible. Measurements of the surface resistance are possible up to temperatures close to T_c, stable sample temperatures of more than 20 K have been established.

SURFACE RESISTANCE CHARACTERIZATION

Method

For measuring the RF surface resistance a calorimetric RF-DC compensation technique is used [8]. The sample is kept at constant temperature where the required DC heater power is recorded with and without RF field inside the resonator. Due to thermal decoupling of sample and resonator, the difference in heater power directly measures the dissipated RF power on the sample surface.

$$P_{\mathrm{diss,\,RF}} = \frac{1}{2}\int_{\mathrm{Sample}} R_s |H|^2 dS = \Delta P_{\mathrm{DC}} \qquad (1)$$

Under the assumption of a uniform surface resistance across the sample the remaining integral of RF magnetic field is directly proportional to the stored energy inside the QPR. Opposed to the QPR already existing at CERN (see e. g. [8] for further details) the resonator is equipped with only one overcoupled input antenna. By using a weakly coupled field probe the peak magnetic field on the sample is given by

$$B_{\mathrm{RF}} = \sqrt{\frac{c_2 Q_t P_t}{2\pi f}} \qquad (2)$$

with the constant c_2 known from simulations and Q_t is the external quality factor of the pickup probe.

The minimum temperature for measurements is given by the helium bath temperature of 1.8 K plus the offset due to RF heating at a given level of field. This offset is typically few 100 mK but can be several Kelvin in case of high surface resistance as observed during measurements at 846 MHz (as one will find in R vs. T data shown later in Fig. 5b).

The available range of RF field level depends on temperature and again on the surface resistance of the sample. The minimum field limit B_{min} is given by the smallest resolvable change in DC heater power. Since the heater power is increasing with temperature and about 1 % of $^{\Delta P_{\mathrm{DC}}}/_{P_{\mathrm{DC}}}$ is required, B_{min} also increases with temperature. In reverse, keeping the RF field constant leads to an increase of measurement error at higher temperature (see points at 10 mT in figures below). The maximum RF field B_{max} is limited typically below the quench limit of the QPR (≈ 120 mT) by RF heating of the sample to temperatures $T > T_{\mathrm{set}}$ and hence the surface resistance. Towards higher temperatures the increase of required DC heater power is typically larger than the RF dissipation due to growing surface resistance, enabling measurements at higher fields (see Figs. 3 and 4).

Data

For every set temperature the reference DC heater power without RF power has to be recorded. For that reason it is quicker to measure surface resistance vs. RF field at constant temperature and to extract $R(T)$ data from those curves afterwards. BCS parameters are obtained by fitting the function

$$R_s(T) = \frac{a}{T}\left(\frac{f}{414\,\mathrm{MHz}}\right)^2 \exp\left(-b\frac{T_c}{T}\right) + R_{\mathrm{res}} \qquad (3)$$

in the temperature range $T < T_c/2$ and with $T_c = 18.5$ K. For the sample discussed in this work surface resistance data is available for temperatures 2 – 10 K and RF fields of 10 – 70 mT at the first two quadrupole modes (414 and 846 MHz).

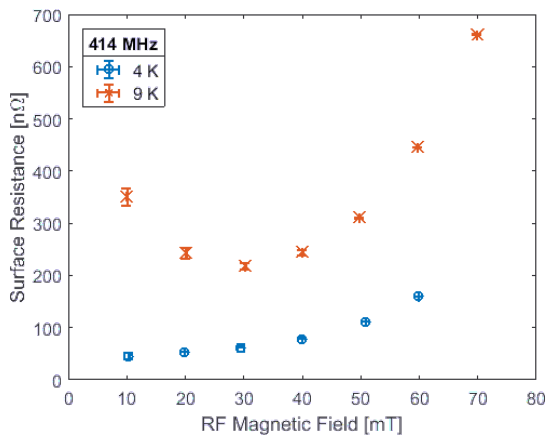

Figure 3: Surface resistance vs. RF field at 414 MHz.

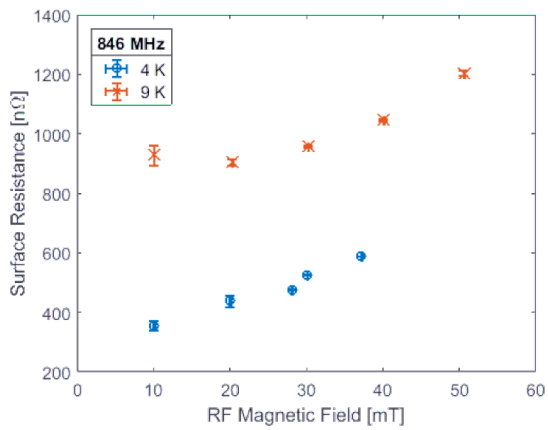

Figure 4: Surface resistance vs. RF field at 846 MHz.

ISBN: 978-3-95450-191-5 doi:10.18429/JACoW-SRF2017-THPB053

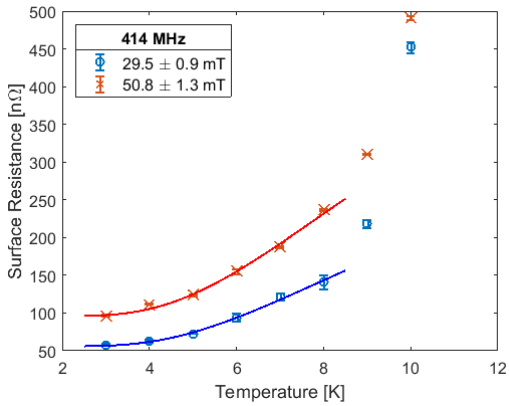

(a) 414 MHz.

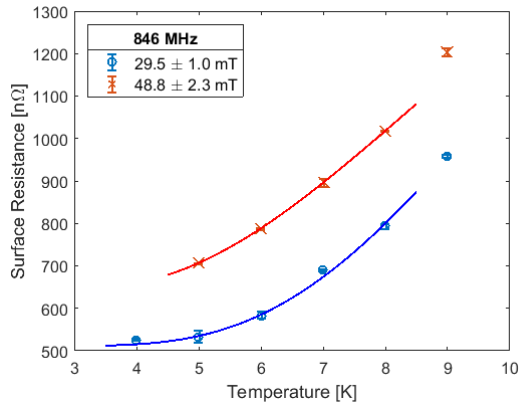

(b) 846 MHz.

Figure 5: R vs. T data extracted from $R(B)$ curves and corresponding BCS fits.

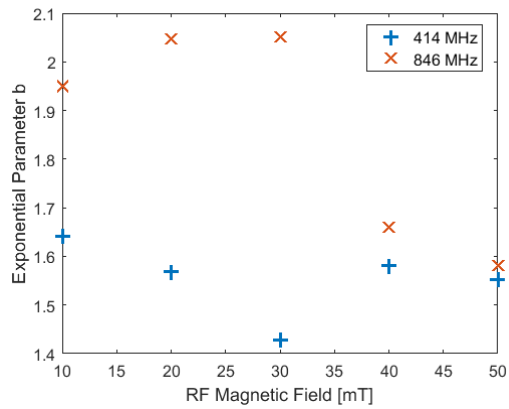

(a) BCS energy gap parameter b.

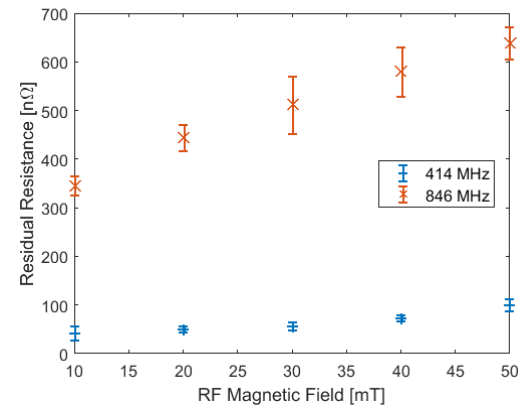

(b) Residual resistance R_{res}.

Figure 6: Results obtained from fitting $R(T)$ curves for different values of RF field and frequencies of 414 and 846 MHz.

Figures 3 and 4 show two data sets for each RF frequency. Note the increasing range of RF field accessible at higher sample temperature. The measurement error increases towards low RF field since the relative change in DC heater power gets very small, especially at high temperature.

Looking at the $R(T)$ curves extracted from this data and the corresponding BCS fits as presented in Figs. 5a and 5b, the impact of high surface resistance on the accessible temperature range is visible. The minimum temperature of a curve is defined by RF heating which allowed measurements at 846 MHz and 50 mT only above 5 K. Due to the very limited number of data points the BCS fits have non-negligible uncertainties. A detailed analysis of the resulting errors is given in [9]. The values of $b = \frac{\Delta}{kT_c}$ as shown in Fig. 6a scatter strongly and only provide an estimate. Nevertheless the residual resistance can be determined within reasonable confidence limits (see Fig. 6b). The residual resistance shows a strong dependence on both frequency and field. The increase with frequency cannot be explained by normal conducting losses $\left(R_{\mathrm{res}} \propto \sqrt{f}\right)$ which also excludes a dominating residual resistance from trapped magnetic flux. From intergrain losses a scaling $R_{\mathrm{res}} \propto f^2$ is expected [1] which could be an explanation but still underestimates the actual scaling factor of 6 – 9. Within the uncertainties of the fitted residual resistance a frequency scaling factor independent of RF field is possible.

RF CRITICAL FIELD

The RF critical field is measured by using pulsed RF at high power. The sample quenches and the transmitted power is recorded with high time resolution [10]. The peak value of transmitted power then corresponds to the quench field of the sample. Stable and repeatable measurements were possible at a field level of 110 mT which is very close to the quench limit of the HZB-QPR.

The temperature dependence of the critical field is expected to be

$$B_c(T) = B_{c,0}\left(1 - \left(\frac{T}{T_c}\right)^2\right) \tag{4}$$

which can be fitted as a straight line in the plot of quench field vs. square of reduced temperature $(T/T_c)^2$ as shown in Fig. 7.

ISBN: 978-3-95450-191-5 doi:10.18429/JACoW-SRF2017-THPB053

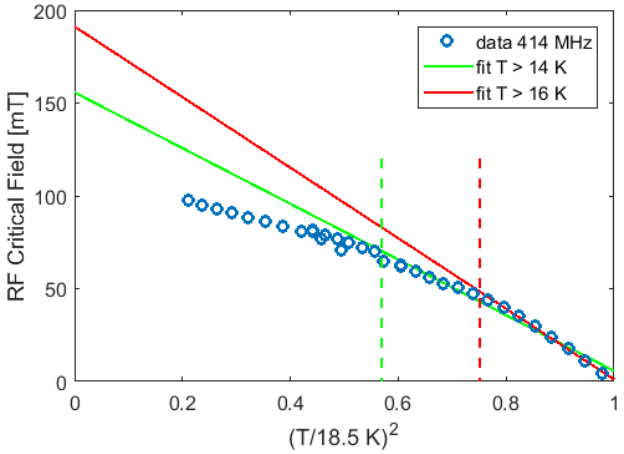

Figure 7: Critical field vs. square of reduced temperature. Red and green line show different temperature ranges used for fitting (14 – 18.5 K and 16 – 18.5 K respectively) which are also indicated by dashed vertical lines.

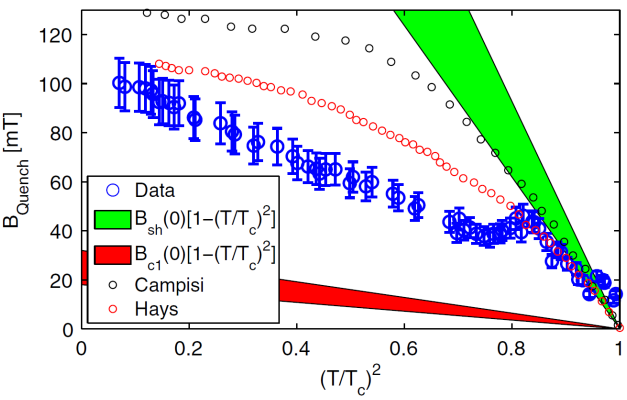

Figure 8: Critical field measured at constant RF power level on a Nb_3Sn single cell cavity. The green area corresponds to $B_{sh} = 390 \pm 80$ mT, $T_c = 18.0 \pm 0.1$ K. Plot taken from [2].

This measurement takes place at constant (maximum) RF power, hence the time it takes to quench the sample increases towards lower temperature. At temperatures below approximately 15 K a deviation from the expected linear trend is observed. This can be explained by RF heating of the sample prior to the quench causing the sample temperature to be systematically underestimated. Current work is ongoing to correct for this effect. Compared to measurements done with a Nb_3Sn single cell cavity at Cornell [2] (see Fig. 8), the critical field observed at temperatures above approximately 16 K is similar. The critical temperature of $T_c = 18.0 \pm 0.1$ K in [2] was obtained from a frequency measurement while the fit in Fig. 7 yields $T_c = 18.5 \pm 0.1$ K for the current data set. This spread in T_c leads to quite different values of B_c extrapolated to 0 K.

CONCLUSIONS

The sample characterized in this work proves the feasibility of the recently developed sample chamber design. This assembly provides a sample holder without stainless steel flange brazed to it enabling high temperature treatments and coatings such as Nb_3Sn. Furthermore samples can be exchanged between the two Quadrupole Resonators available at CERN and HZB.

Surface resistance measurements up to 70 mT and at frequencies of 414 and 846 MHz showed high residual resistance but critical temperature and superconducting energy gap as expected. Especially the high critical temperature of about 18.5 K indicates a successful coating with Nb_3Sn and good stoichiometry. The measured RF critical field of $B_c \approx 190$ mT is only about half of the expected superheating field ($B_{sh} \approx 400$ mT) but far above B_{c1}.

ACKNOWLEDGEMENTS

The research leading to these results has received funding from the European Commission under the FP7 Research Infrastructures project EuCARD-2, grant agreement No. 312453.

The Cornell part of this work was supported by U.S. DOE award DE-SC0008431.

REFERENCES

[1] H. Padamsee, J. Knobloch, and T. Hays, *RF Superconductivity for Accelerators*, John Wiley & Sons, Inc., New York, 1998.

[2] S. Posen and M. Liepe, *Phys. Rev. ST Accel. Beams* 17, 112001 (2014).

[3] M. Liepe and S. Posen, "Nb_3Sn for SRF Application", in *Proc. SRF'13*, Paris, France, 2013.

[4] R. Kleindienst, "Radio Frequency Characterization of Superconductors for Particle Accelerators", PhD thesis, submitted to University of Siegen, 2017.

[5] E. Mahner, S. Calatroni, E. Chiaveri, E. Haebel, and J. M. Tessier, *Rev. Sci. Instrum.* 74, 3390 (2003).

[6] R. Kleindienst, O. Kugeler, and J. Knobloch, "Development of an Optimized Quadrupole Resonator at HZB", in *Proc. SRF'13*, Paris, France, 2013.

[7] R. Kleindienst, A. Burrill, S. Keckert, J. Knobloch, and O. Kugeler, "Commissioning Results of the HZB Quadrupole Resonator", in *Proc. SRF'15*, Whistler, Canada, 2015.

[8] T. Junginger, W. Weingarten, and C. Welsch, "Review of RF-Sample Test Equipment and Results", in *Proc. SRF'11*, Chicago, USA, 2011.

[9] S. Keckert, O. Kugeler, and J. Knobloch, "Error Analysis of Surface Resistance Fits to Experimental Data", presented at SRF'17, Lanzhou, China, July 2017, paper THPB052, this conference.

[10] F. Kramer, "Messung des kritischen Magnetfelds von supraleitenden Proben in Hochfrequenzfeldern", B. Sc. thesis, University of Siegen, 2017.